

Proceedings of XIX International Scientific Conference “New Technologies and Achievements in Metallurgy, Material Engineering, Production Engineering and Physics”, Częstochowa, Poland, June 7–8, 2018

The Magnetic, Structural and Electronic Properties of Novel Y_2FeSi Full-Heusler Alloy

K. GRUSZKA* AND K. BEDNARSKA

Institute of Physics, Częstochowa University of Technology, 42-200 Częstochowa, Poland

The paper presents the results of the plane wave density functional theory calculations of newly predicted Y_2FeSi full-Heusler alloy with optimized lattice constants. We have explored two most likely structures (AlCu₂Mn and CuHg₂Ti prototypes) with different atomic arrangements and including collinear magnetic ordering. The results show that the classic $L2_1$ structure is more favourable in terms of energy than the second one studied in this work. Moreover, for both crystalline structures ferromagnetic arrangement is more favourable, although in the second structure the difference in energy between ferromagnetic and nonmagnetic state is small. Study did not revealed band gap in any spin channel, yet the spin polarization in majority channel at the Fermi level is significant ($\sigma = 83\%$). The calculated structural lattice a parameter for the energetically lowest structure is $a = 13.0996 a_0$. For the lattice constant range of 12.2 to 13.2 a_0 the total magnetic moment varies significantly from 0.86 μ_B to 1.74 μ_B per formula unit.

DOI: [10.12693/APhysPolA.135.107](https://doi.org/10.12693/APhysPolA.135.107)

PACS/topics: 02.70.-c, 13.40.Em, 71.15.Mb, 71.20.-b

1. Introduction

Recently, both half-Heusler (HH) and full-Heusler (FH) materials have attracted a lot of attention due to their excellent properties that include half metallic state and magnetic ordering, in the same time. Those properties result in their potential application in spintronic devices such as spin-filters [1] or spin injection devices [2, 3]. However, to adjust parameters of such materials, a basic knowledge at the lowest atomic level is required, especially focused on its electronic properties. The electronic structure of FH and HH materials is inextricably linked to its crystallographic structure, thus changing the atomic site occupations will significantly influence materials various properties, despite the same chemical composition.

The full-Heusler alloys of the X_2YZ composition (where X and Y are elements from transition metal d -orbital block and Z is sp -orbital element from p block [4]) crystallize in one of two main structures, namely $L2_1$ (AlCu₂Mn-type) and CuHg₂Ti-type. The final structure in which material crystallizes depends on the overall energy which it can obtain by choosing one of them. Here many properties affect this energy like the range of electron orbital clouds overlapping or magnetic ordering, to name few. This properties can be determined based on experiments (such as X-ray diffraction (XRD) or vibrating sample magnetometer (VSM)) when material sample is available or by *ab initio* approach using various calculation methods [5–8]. The latter one gives full information about material intrinsic interactions, allowing to predict and better understand of its properties.

In this paper, the magnetic structural and electronic properties of novel Y_2FeSi full-Heusler alloy are determined using density functional theory (DFT) calculations.

2. Computational details

The calculations were completed using Quantum Espresso software package [9]. Both geometrical optimization and electronic structure calculations were performed using DFT which were carried out by the means of plane wave method. The generalized gradient approximation (GGA) in the Perdew, Burke, and Ernzerhof (PBE) form were used [10]. For all calculations the projector augmented-wave (PAW) pseudopotentials were used. The electronic configurations for Y, Si, and Fe elements were [Kr] $5s^2 5p^0 4d^1$, [Ne] $3s^2 3p^2 3d^0$, and [Ar] $4s^2 3d^6 4p^0$, respectively. When considering $L2_1$ structure (space group $Fm-3m$, no. 225) the Y occupies 8c ($\frac{1}{4}, \frac{1}{4}, \frac{1}{4}$), Si — 4b ($\frac{1}{2}, \frac{1}{2}, \frac{1}{2}$) and Fe — 4a (0,0,0) prototype AlCu₂Mn. For the second Heusler structure of CuHg₂Ti prototype ($F-43m$, no. 216), Y atom occupies 4a (0,0,0) and 4c ($\frac{1}{4}, \frac{1}{4}, \frac{1}{4}$), Si — 4d ($\frac{3}{4}, \frac{3}{4}, \frac{3}{4}$) and Fe — 4b ($\frac{1}{2}, \frac{1}{2}, \frac{1}{2}$) sites. All computations were done including scalar relativistic effects. Before final calculations to ensure accurate results we conducted proper convergence tests. On that base, we established a $17 \times 17 \times 17$ k -points mesh aligned in the Monkhorst–Pack scheme [11] for sampling of the Brillouin zone. The kinetic energy cutoff was set to $ecutwfc = 90$ Ry (0.1224×10^4 eV) and cutoff for charge density $ecutrho = 900$ Ry (1.2245×10^4 eV). To properly treat metallic materials and accelerate the convergence Marzari–Vanderbilt [12] cold smearing of the Fermi surface with value of 0.005 Ry (0.068 eV) was used. The electronic convergence criteria was set to 10^{-8} Ry (1.36×10^{-7} eV). For the relaxation procedures,

*corresponding author; e-mail: kgruszka@wip.pcz.pl

the total force threshold for ionic minimization was set to 1×10^{-3} a.u. and kinetic stress for equilibrated structure below 0.1 kPa. All relaxation calculations were done including proper magnetic ordering when needed, two options were considered: non-magnetic (NM) case and ferromagnetic (FM) spin ordering for both investigated structures.

3. Results and discussion

Figure 1 shows both considered structures of Y_2FeSi material. At first stage the structural properties (equilibrium lattice constant) were calculated for all the structures using classic minimization of energy in respect of cubic lattice parameter a and substituting results to the Murnaghan equation of state [13] (see Fig. 2, Eq. (1)). Then we utilized the Broyden–Fletcher–Goldfarb–Shanno (BFGS) algorithm to further improve accuracy and relax the ionic positions inside the cell. The cell parameters data for both structures resulted from last step have been summarized in Table I.

As can be seen, the most energetically stable configuration is ferromagnetic $Fm-3m$ ($L2_1$). For the second investigated structure, both FM and NM states show similar behaviour. In this case the calculation showed that attempt to enforce a ferromagnetic order-

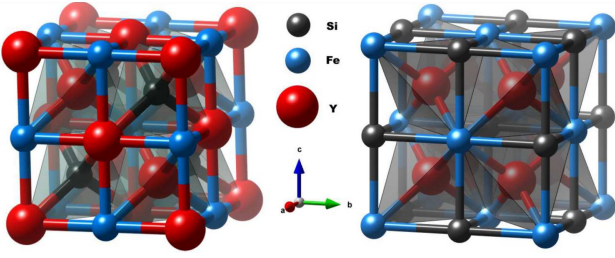


Fig. 1. The $F-43m$, $CuHg_2Ti$ type (left) and $Fm-3m$, $AlCu_2Mn$ type (right) Heusler structures.

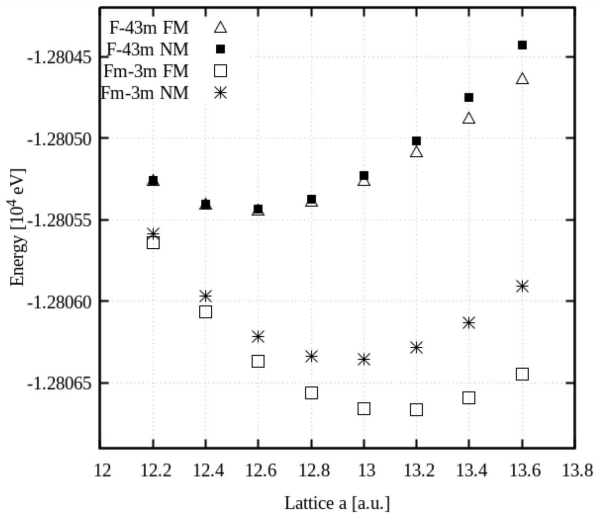


Fig. 2. Total energy in function of lattice a parameter.

TABLE I

Structural parameters for investigated configurations.

Structure	Y_2FeSi	a lattice parameter [a.u.]	Volume [a.u. ³]	Density [g/cm ³]	Total energy [eV]
$Fm-3m$	FM	13.09958	561.9686	5.218	-12806.67186
	NM	12.92950	540.3624	5.425	-12806.36365
$F-43m$	FM	12.57045	496.5837	5.904	-12805.44116
	NM	12.56100	495.4646	5.898	-12805.43805

ing strives for non-magnetic configuration during SCF (Self-Consistent Field) cycles. Because the $L2_1$ structure is more favourable, the following part of the article will refer to this phase exclusively.

From the fit of energy-volume curve to the Murnaghan Eq. (1) the bulk modulus can be calculated. For the $L2_1$ FM structure we report its value to be $B = 75.9$ GPa.

The used Murnaghan equation of state is given by

$$E(V) = E_0 + \frac{K_0 V}{K'_C} \left(\frac{(V_0/V)^{K'_0}}{K'_0 - 1} + 1 \right) - \frac{K_0 V_0}{K'_0 - 1}, \quad (1)$$

where K_0 — bulk modulus, K'_0 — derivative of K_0 , E_0 — equilibrium energy, V_0 — equilibrium volume, V — volume.

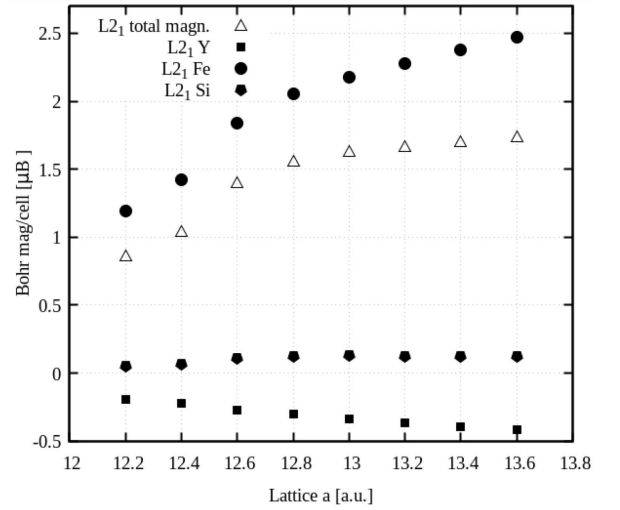


Fig. 3. Total and local magnetic moments in function of lattice a parameter for $L2_1$ ($Fm-3m$) structure.

Figure 3 shows change of total and local magnetic moments for Y_2FeSi in $L2_1$ FM configuration in respect of lattice a parameter. The total magnetic moment is defined as:

$$\int (n_{up} - n_{down}) d^3r, \quad (2)$$

Where n_{up} and n_{down} are magnetic moments coming up from spin up and down, respectively. The calculated total magnetic moment for relaxed structure is $1.56 \mu_B/\text{cell}$. As can be seen, total magnetic moment rises with rising a up to 12.8 a.u. and, above this value, increase of μ_B is smaller but still visible. The main contribution to total magnetization is caused by Fe site with very small

addition of silicon moment. At the same time both yttrium sites are polarised anti-parallel to the iron, lowering the total magnetization.

Below 12.8 a.u. as the cell compression increases, a sharp decrease in total magnetization can be seen. This is mainly caused by drop of Fe local moment, which behaves similarly in this range and two yttrium sites aligned anti-parallel. A very slight drop of Si from $0.1253 \mu_B$ at $a = 12.8$ to $0.1212 \mu_B$ at $a = 12.2$ a.u. can also be observed. At $a = 12.2$ a.u. (which corresponds to 2.38 GPa of hydrostatic pressure) the total magnetic moment drops to $0.86 \mu_B$, almost twice smaller when compared to equilibrium lattice constant.

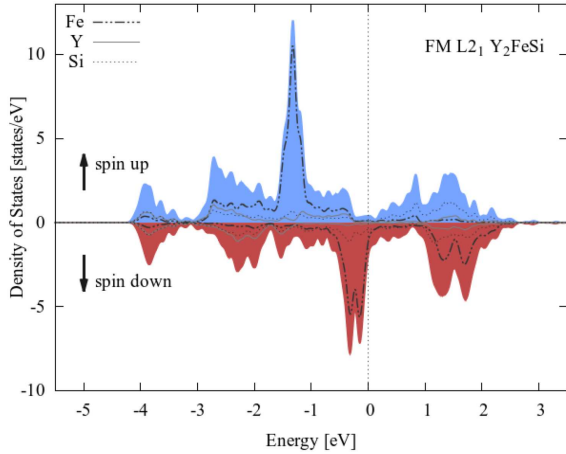


Fig. 4. Total and projected density of states for $L2_1$ FM configuration. The Fermi level is placed at 0 eV.

Figure 4 presents total and atom-projected density of states for Y_2FeSi in $L2_1$ FM configuration. As can be seen, at about -0.25 eV below the Fermi level in spin down channel high peak from Fe ion (and partial Si contribution) emerges, a characteristic feature of ferromagnetic ordering. In general, total DOS (shown in red and blue) comes in the majority from iron states contribution (in the spin up channel, up to the Fermi level, and above Fermi in spin down channel). The lower lying states in spin down channel (from -4 to -1.5 eV) originate from yttrium and silicon mixed states. At the Fermi level there are significantly less available states coming from spin up channel than spin down channel. The calculated spin polarization at $E_F \sigma \approx 83\%$ is high, which opens up possibilities for use in spin filter devices. This polarization at E_F comes largely from Fe ion states, therefore it confirms that total cell magnetization comes mainly from iron sites. Also, because the considerable share of Si states at E_F are also contributing to spin down channel, it suggests that while increasing the a lattice constant the induced opposing magnetic moment observed in Fig. 3 comes from Y ions, which is also confirmed.

4. Conclusions

In this paper we studied structural, magnetic and electronic properties of novel full-Heusler Y_2FeSi material.

As the results have shown, the most energetically stable configuration from those considered both with non-magnetic and ferromagnetic spin arrangement is the $L2_1$ with ferromagnetic spin ordering. The magnetic properties are strongly related to the crystal structure, causing an increase in the total magnetic moment as the cell size increases beyond equilibrium, and a sharp drop, when cell is compressed. However, despite of the increase in total magnetization the decrease in local moment of Y ions are also observed, therefore an imbalance resulting from opposite magnetic moments exists. The low influence of Si local moment is stable in studied range. For the second investigated structure ($CuHg_2Ti$ prototype) at equilibrium, materials magnetization drops to zero.

The electronic structure calculations (atom-projected density of states) showed that for equilibrium lattice constant of $a = 13.0996$ a.u. for $L2_1$ ferromagnetic structure, main contribution to the DOS at the Fermi level and therefore to total magnetic moment ($1.56 \mu_B$) comes from iron ions. High spin polarization of $\sigma = 83\%$ opens up application possibilities for use in spin filter or spin injection devices.

References

- [1] M. Tas, E. Şaşıoğlu, C. Friedrich, I. Galanakis, *J. Magn. Magn. Mater.* **441**, 333 (2017).
- [2] Yue Wang, Xiaoming Zhang, Bei Ding, Zhipeng Hou, Enke Liu, Zhongyuan Liu, Xuekui Xi, Hongwei Zhang, Guangheng Wu, Wenhong Wang, *Computat. Mater. Sci.* **150**, 321 (2018).
- [3] Ch.J. Palmstrøm, *Progr. Cryst. Growth Character. Mater.* **62**, 371 (2016).
- [4] K. Gruszka, M. Szota, M. Nabiałek, *Rev. Chim.* **68**, 487 (2017).
- [5] K. Gruszka, M. Nabiałek, T. Noga, *Archiv. Metall. Mater.* **61**, 369 (2016).
- [6] A. Esmaeili, M.H. Entezari, E.K. Goharshadi, *Appl. Surf. Sci.* **451**, 112 (2018).
- [7] Y. Takahara, *Mater. Sci. Eng. A* **231**, 128 (1997).
- [8] Saeed Nasiri, Mansour Zahedi, *Chem. Phys. Lett.* **634**, 101 (2015).
- [9] P. Giannozzi, S. Baroni, N. Bonini, M. Calandra, R. Car, C. Cavazzoni, D. Ceresoli, G.L. Chiarotti, M. Cococcioni, I. Dabo, A. Dal Corso, S. de Gironcoli, S. Fabris, G. Fratesi, R. Gebauer, U. Gerstmann, Ch. Gougoussis, A. Kokalj, M. Lazzeri, L. Martin-Samos, N. Marzari, F. Mauri, R. Mazzarello, S. Paolini, A. Pasquarello, L. Paulatto, C. Sbraccia, S. Scandolo, G. Sciauzero, A.P. Seitsonen, A. Smogunov, P. Umari, R.M. Wentzcovitch, *J. Phys. Condens. Matter.* **21**, 395502 (2009).
- [10] J.P. Perdew, K. Burke, M. Ernzerhof, *Phys. Rev. Lett.* **77**, 3865 (1996).
- [11] J.H.J. Monkhorst, J.D. Pack, *Phys. Rev. B* **13**, 5188 (1976).
- [12] N. Marzari, D. Vanderbilt, A. De Vita, M.C. Payne, *Phys. Rev. Lett.* **82**, 3296 (1999).
- [13] F. Birch, *Phys. Rev.* **71**, 809 (1947).